

Supporting Information

2.6 V Aqueous Symmetric Supercapacitors Based on the Phosphorus-doped TiO₂

Nanotube Arrays

Yaxiong Zhang^{a,b,1}, Shifang Duan^{c,1}, Yan Li^{a,b}, Shengming Zhang^{a,b}, Yin Wu^{a,b},

Mingyu Ma^{a,b}, Chunlan Tao^d, Zhenxing Zhang^{a,b,*}, Dongdong Qin^{d,*}, Erqing Xie^{a,b}

^a School of Physical Science and Technology, Lanzhou University, Lanzhou 730000,
China

^b Key Laboratory for Magnetism and Magnetic Materials of the Ministry of Education,
Lanzhou University, Lanzhou 730000, China

^c College of Chemistry and Chemical Engineering, Northwest Normal University,
Lanzhou 730070, People's Republic of China

^d College of Chemistry and Chemical Engineering, Guangzhou University,
Guangzhou 510006, People's Republic of China

¹ These authors contribute equally

* Corresponding authors:

E-mail: zhangzx@lzu.edu.cn (Z Z),

E-mail: ccqindd@gzhu.edu.cn (D Q)

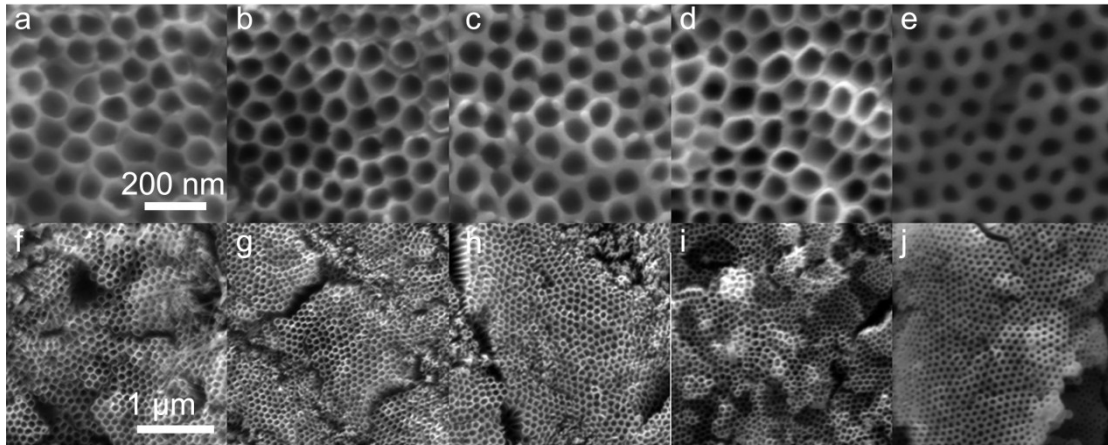


Fig. S1 SEM images of TP-300 TP-400, of TP-500, TP-600, and T-700 at high and low magnifications. There are no obvious changes from high and low magnified SEM images.

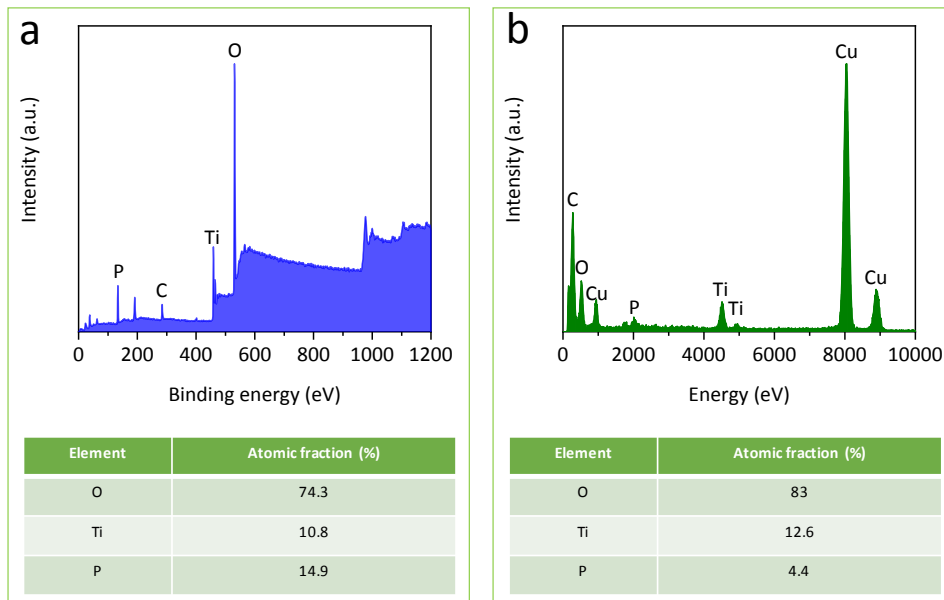


Fig. S2 TP-600 sample: (a) the XPS spectra and the atomic fraction; (b) the EDS and the atomic fraction.

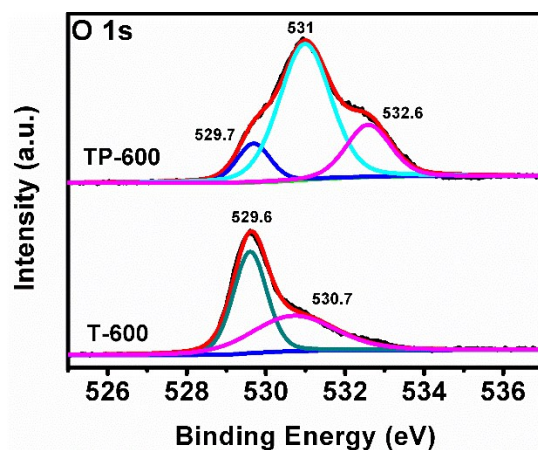


Fig. S3 O 1s core-level XPS spectra of the TP-600 and T-600 samples.

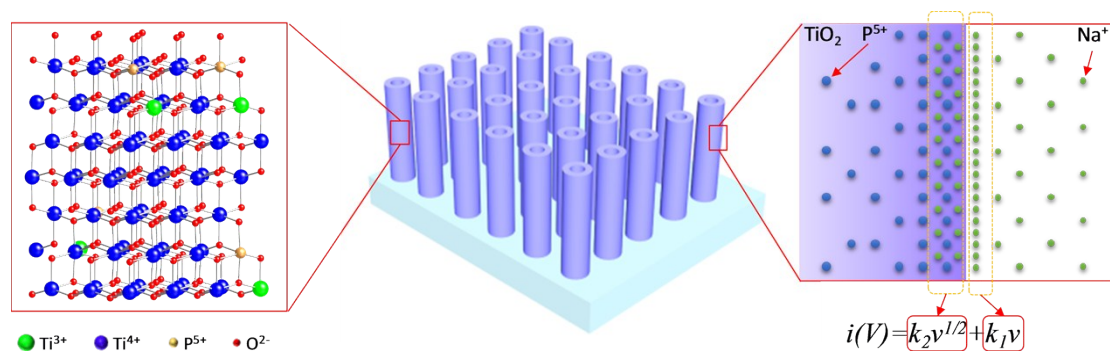


Fig. S4 Schematic illustration of the status of doped P and the electrochemical reaction of the electrode.

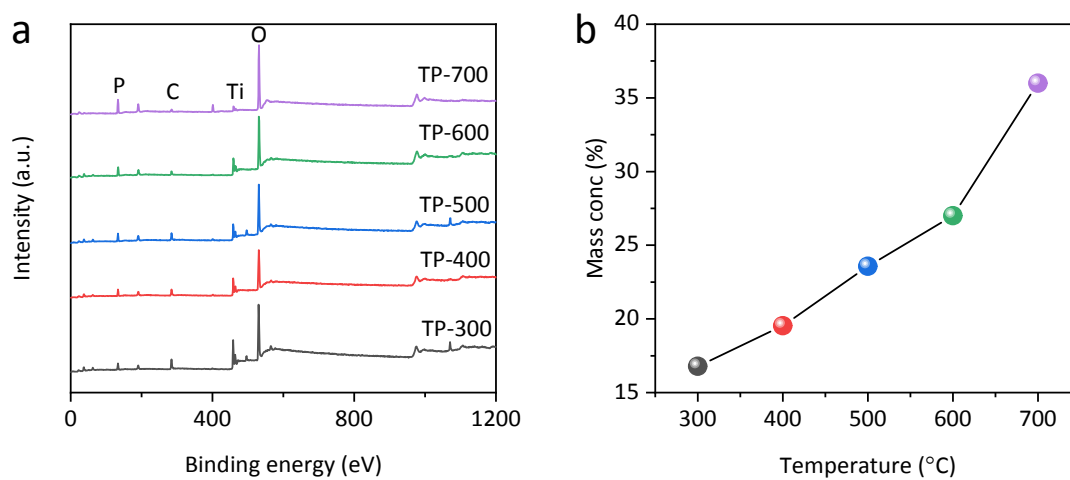


Fig. S5 (a) XPS and (b) P content of the P-doped TiO₂ nanotube arrays prepared at

different temperatures.

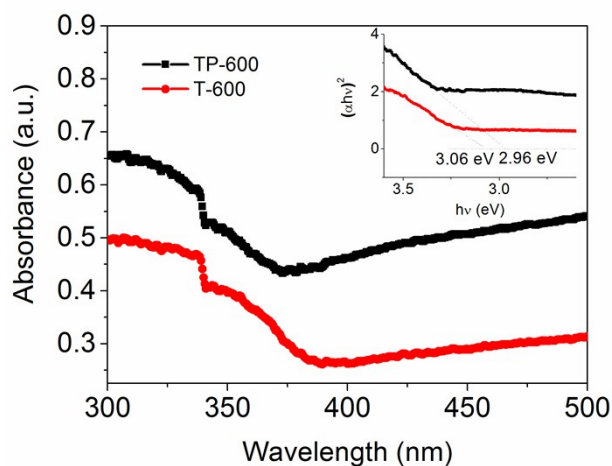


Fig. S6 UV-Visible spectroscopy of TP-600 and T-600.

The UV–visible spectra of TP-600 and T-600 are shown in **Fig. S6**. They showed a weak absorption in the range of 300-500 nm. The energy of the band gap of the TP-600 and T-600 samples could be calculated by the following equation: [1]

$$\alpha h\nu = A(h\nu - E_g)^{1/2}$$

Where α , $h\nu$, A , and E_g are the optical absorption coefficient, energy of the incident photon, proportionality constant, and band gap energy, respectively. The inset in Fig. S6 shows the plot of $(\alpha h\nu)^2$ versus $h\nu$, and the band gap energies calculated from the intercept of the tangent of the plot are 2.96 eV of TP-600 and 3.06 eV of T-600.

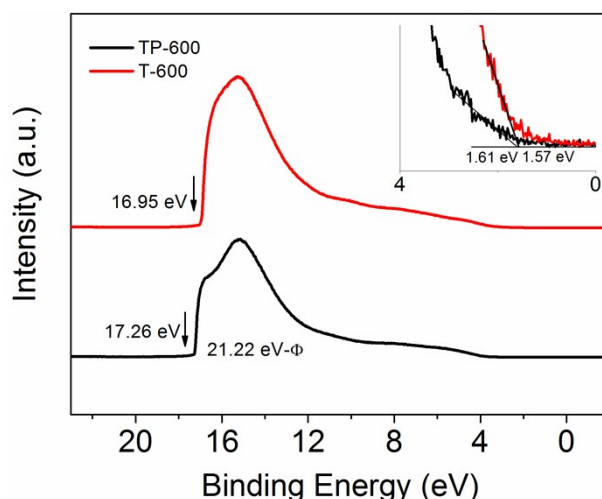


Fig. S7 UPS spectra of TP-600 and T-600.

From the UPS spectra, the secondary electron cutoff edge (left vertically downward arrow) and the valence band edge (right) can be found. Due to the very sharp secondary electron cutoff edge, the work function can be directly obtained from the spectra by subtracting the binding energy of the secondary electron cutoff from the excitation energy of Helium source (21.22 eV). In the UPS spectra of the TP-600 and T-600 samples, the secondary electron cutoff are 17.26 eV and 16.95 eV. Thus, the work functions of TP-600 and T-600 are 3.96 and 4.27 eV, respectively.

Because the valence band edge is gentle, the valence band maximum (E_V) cannot be obtained directly by UPS spectra. The linear extrapolation of the leading edge to the extended baseline of the valence band spectra is used to calculate the position of E_V (inset in **Fig. S7**). That means the E_V is the intersection's abscissa of the extension line of the valence band leading edge and the background channel. The deduced E_V of TP-600 and T-600 are 1.61 eV and 1.57 eV, respectively.[2, 3]

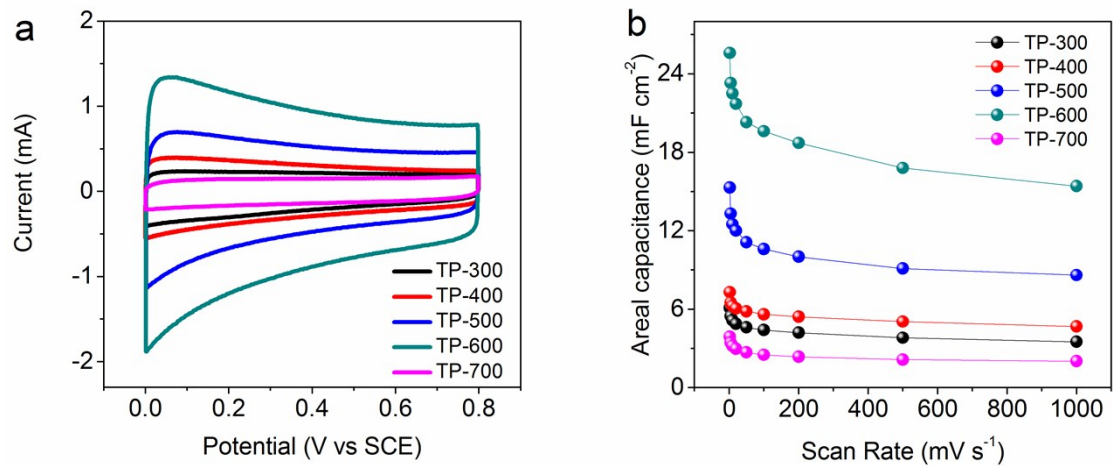


Fig. S8 TP-300 TP-400, TP-500, TP-600, and TP-700 samples: (a) CV curves; (b) areal capacitance versus scan rate.

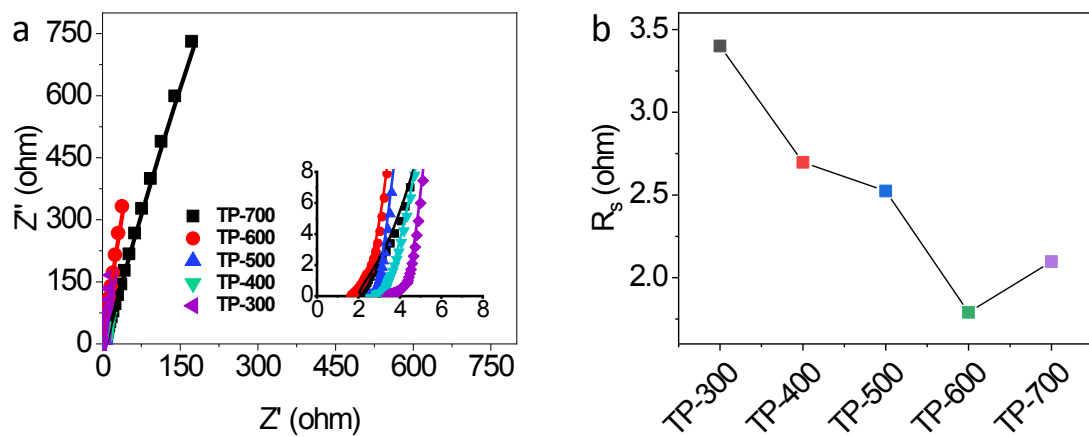


Fig. S9 P-doped TiO₂ nanotube arrays prepared at different temperatures: (a) Nyquist plots and the fitting plots; (b) The deduced R_s from EIS.

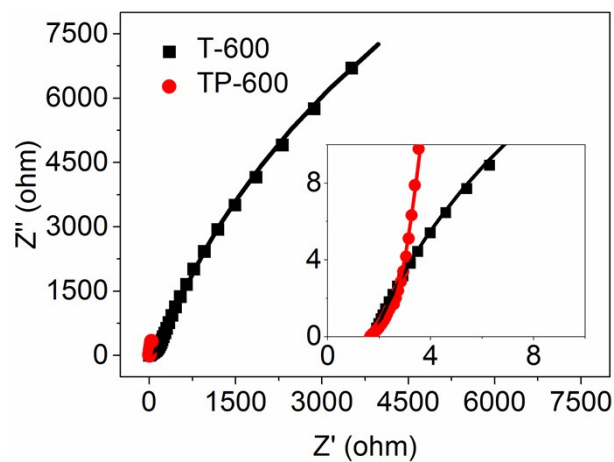


Fig. S10 Nyquist and fitted plots of the TP-600 and T-600 samples.

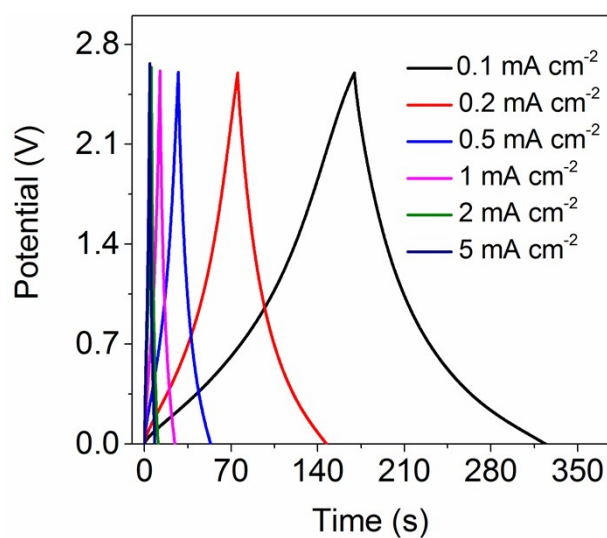
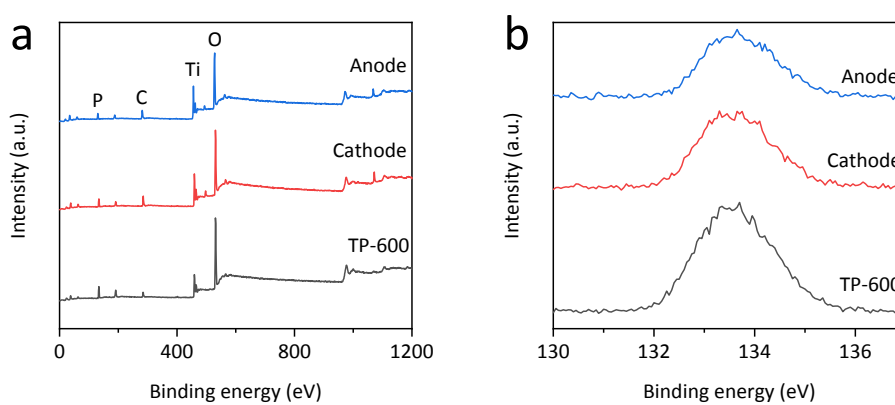


Fig. S11 The GCD curves of device at different current densities.



| Element | TP-600 Atomic fraction (%) | Cathode Atomic fraction (%) | Anode Atomic fraction (%) |
|---------|----------------------------|-----------------------------|---------------------------|
| O | 74.3 | 71.6 | 71.5 |
| Ti | 10.8 | 16.42 | 17.6 |
| P | 14.9 | 11.98 | 10.9 |

Fig. S12 (a) XPS spectra of the pristine TP-600, the TP-600 samples as positive and negative electrodes after cycling; (b) the corresponding P core-level XPS spectra and atomic fraction of (a).

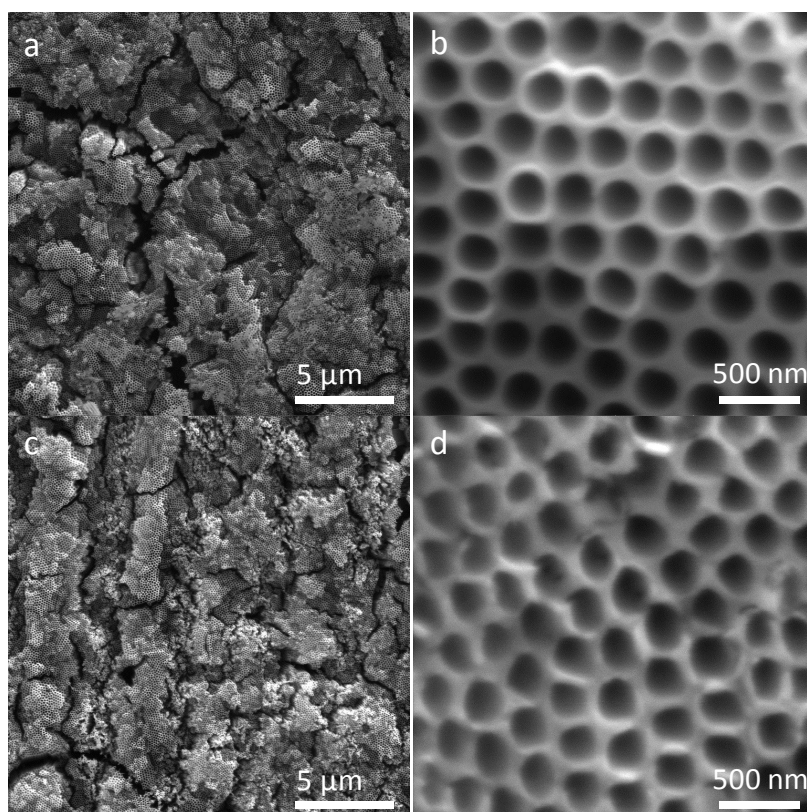


Fig. S13 SEM images of the TP-600 sample as positive (a and b) and negative (c and d) electrode after 10000 charging-discharging cycles. There is no obvious change in high and low magnified SEM images between the sample after cycle and the original sample.

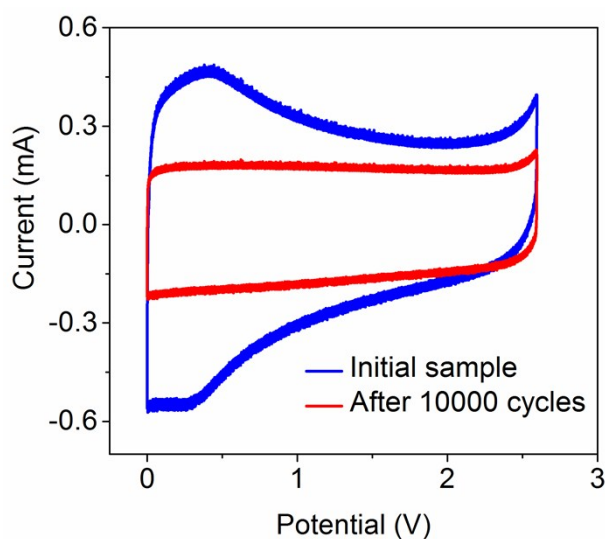


Fig. S14 CV curves of the device before and after 10000 cycles

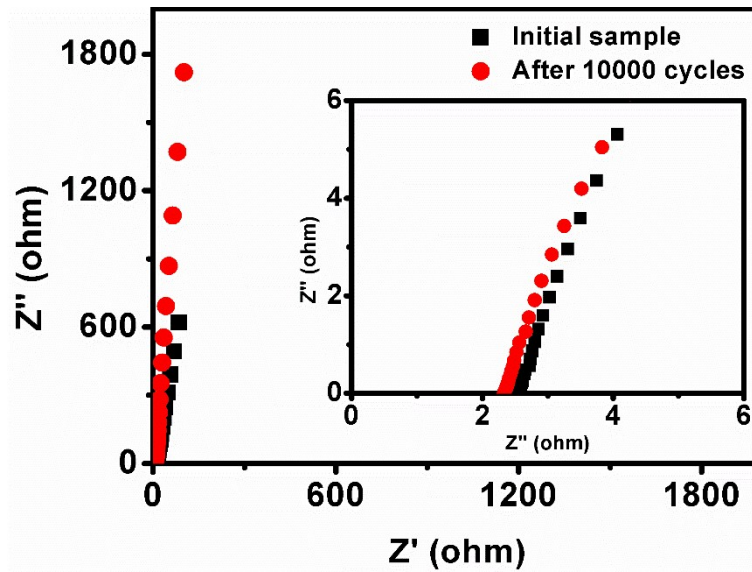


Fig. S15 Nyquist plots of the device before and after 10000 cycles.

References:

- [1] Walsh A, Da Silva JL, Wei SH, Korber C, Klein A, Piper LF, et al., Nature of the band gap of In_2O_3 revealed by first-principles calculations and x-ray spectroscopy, *Phys Rev Lett* 100(2008) 167402.
- [2] King PDC, Veal TD, Jefferson PH, McConville CF, Wang T, Parbrook PJ, et al., Valence band offset of InN/AlN heterojunctions measured by x-ray photoelectron spectroscopy, *Applied Physics Letters* 90(2007) 132105.
- [3] Klein A, Green DJ, Transparent Conducting Oxides: Electronic Structure-Property Relationship from Photoelectron Spectroscopy within situ Sample Preparation, *Journal of the American Ceramic Society* (2012) n/a-n/a.